Prostaglandin dehydrogenase is a target for successful induction of cervical ripening

Annavarapu Hari Kishore[a], Hanquan Liang[b], Mohammed Kanchwala[b], Chao Xing[b,c], Thota Ganesh[d], Yucel Akgul[e], Bruce Posner[f,g], Joseph M. Ready[f,g], Sanford D. Markowitz[h,i,j], and Ruth Ann Word[a,1]

[a]The Cecil H. and Ida Green Center for Reproductive Biology, Department of Obstetrics and Gynecology, University of Texas Southwestern Medical Center, Dallas, TX 75390; [b]Eugene McDermott Center for Human Growth & Development and Department of Bioinformatics, University of Texas Southwestern Medical Center, Dallas, TX 75390; [c]Department of Clinical Sciences, University of Texas Southwestern Medical Center, Dallas, TX 75390; [d]Department of Pharmacology, Emory University School of Medicine, Atlanta, GA 30322; [e]Department of Plastic Surgery, University of Texas Southwestern Medical Center, Dallas, TX 75390; [f]Department of Biochemistry, University of Texas Southwestern Medical Center, Dallas, TX 75390; [g]Simmons Cancer Center, University of Texas Southwestern Medical Center, Dallas, TX 75390; [h]Department of Medicine, Case Western Reserve University, Cleveland, OH 44106; [i]Case Comprehensive Cancer Center, Case Western Reserve University, Cleveland, OH 44106; and [j]Seidman Cancer Center, University Hospitals of Cleveland, Cleveland, OH 44106

Edited by Catalin S. Buhimschi, The Ohio State University College of Medicine, and accepted by Editorial Board Member R. M. Roberts June 21, 2017 (received for review March 27, 2017)

The cervix represents a formidable structural barrier for successful induction of labor. Approximately 10% of pregnancies undergo induction of cervical ripening and labor with prostaglandin (PG) E_2 or PGE analogs, often requiring many hours of hospitalization and monitoring. On the other hand, preterm cervical ripening in the second trimester predicts preterm birth. The regulatory mechanisms of this paradoxical function of the cervix are unknown. Here, we show that PGE_2 uses cell-specific EP2 receptor-mediated increases in Ca^{2+} to dephosphorylate and translocate histone deacetylase 4 (HDAC4) to the nucleus for repression of 15-hydroxy prostaglandin dehydrogenase (15-PGDH). The crucial role of 15-PGDH in cervical ripening was confirmed in vivo. Although PGE_2 or 15-PGDH inhibitor alone did not alter gestational length, treatment with 15-PGDH inhibitor + PGE_2 or metabolism-resistant dimethyl-PGE_2 resulted in preterm cervical ripening and delivery in mice. The ability of PGE_2 to selectively autoamplify its own synthesis in stromal cells by signaling transcriptional repression of *15-PGDH* elucidates long sought-after molecular mechanisms that govern PG action in the cervix. This report details unique mechanisms of action in the cervix and serves as a catalyst for (*i*) the use of 15-PGDH inhibitors to initiate or amplify low-dose PGE_2-mediated cervical ripening or (*ii*) EP2 receptor antagonists, HDAC4 inhibitors, and 15-PGDH activators to prevent preterm cervical ripening and preterm birth.

prostaglandin E_2 | cervical shortening | preterm labor | labor induction | HDAC4

Despite decades of clinical use for cervical ripening and induction of labor, mechanisms of prostaglandin (PG)-mediated cervical ripening are largely unknown. Likewise, it is not understood why some women at term respond to vaginal PGs for cervical ripening whereas others do not. Although failure rates vary depending on preparation, method of administration, definition of failure, dose, and dosing interval, in general the overall risk of the cervix remaining unchanged or unfavorable for induction of labor 12–24 h after vaginal PGs is 21.6% (1), which is consistent with a recent report in which 122 of 488 (25%) women failed to obtain a ripe cervix (as defined by Bishop Score < 7) after 4 PGE_2 (3 mg) tablets (2). Further, PGE_2 treatment leads to uterine hyperstimulation in 1–5.8%, of which 31% are associated with abnormalities in fetal heart rhythm (3). Both problems require emergency treatment and, in many cases, urgent operative delivery.

Increased endogenous cervical PGs are derived from increased expression of the enzyme cyclooxygenase-2 (COX-2), which converts arachidonic acid to PGH_2, which is then converted by PGE synthase (PTGES) to PGE_2. Increases in cervical PGE_2 are prevented not only by low levels of COX-2 but also by high levels of the enzyme 15-prostaglandin dehydrogenase (15-PGDH) that inactivates PGE_2 by converting it to inactive 15-keto-PGE_2 (4–6). Hence, tissue levels of PGE_2 are regulated by the relative abundance of COX-2 and 15-PGDH enzymes. COX-2 levels increase in the cervix at term and in the myometrium and cervix of women with infection (7) or in preterm labor (8–10). COX-2 inhibitors inhibit preterm labor (11, 12). In contrast to COX-2, 15-PGDH levels are decreased in the ripe cervix at term relative to the high levels of this enzyme before cervical ripening (6). Together, these studies indicate that COX-2 and 15-PGDH are inversely correlated in the human cervix, thereby regulating the relative abundance of cervical PGE_2 and cervical ripening.

Dinoprostone (PGE_2) and misoprostol (PGE_1 analog) are commonly used to induce cervical ripening in women at term. PGE_2 acts through four receptors (EP1, EP2, EP3, and EP4) expressed at different relative levels, thereby directing PGE_2 signaling in various cell types. Our studies have shown that EP2 receptor expression is remarkably enriched in human cervical stromal tissues relative to EP1, EP3, or EP4 (5). Further, experimental

Significance

Prostaglandin E_2 (PGE_2), a cervical ripening agent, mediates unique EP2 receptor signaling pathways in human cervical stromal cells targeting its own synthesis by increasing cyclooxygenase-2 (COX-2) and PGE synthase (PTGES) expression and decreasing its metabolism by loss of its degradative enzyme 15-hydroxy prostaglandin dehydrogenase (15-PGDH). Here, we show that down-regulation of 15-PGDH is crucial for PGE_2-induced cervical ripening and preterm birth. This report details unique mechanisms of PGE_2 action in the cervix and serves as a catalyst for (*i*) use of PGDH inhibitors to initiate, or amplify, PGE_2-mediated cervical ripening and (*ii*) EP2 receptor antagonists, histone deacetylase 4 (HDAC4) inhibitors, or 15-PGDH activators to prevent preterm cervical ripening and preterm birth.

Author contributions: A.H.K. and R.A.W. designed research; A.H.K. performed research; Y.A. performed confocal microscopy; A.H.K., T.G., B.P., J.M.R., and S.D.M. contributed new reagents/analytic tools; A.H.K., H.L., M.K., C.X., and R.A.W. analyzed data; and A.H.K. and R.A.W. wrote the paper.

The authors declare no conflict of interest.

This article is a PNAS Direct Submission. C.S.B. is a Guest Editor invited by the Editorial Board.

Data deposition: The data reported in this paper have been deposited in the Gene Expression Omnibus (GEO) database, https://www.ncbi.nlm.nih.gov/geo (accession no. GSE99392).

[1]To whom correspondence should be addressed. Email: ruth.word@utsouthwestern.edu.

This article contains supporting information online at www.pnas.org/lookup/suppl/doi:10.1073/pnas.1704945114/-/DCSupplemental.

evidence indicates that PGE_2 acts specifically through EP2 receptors in a cAMP-independent manner in these cells to repress 15-PGDH gene expression (5). Nonetheless, the downstream cellular signaling pathways of PGE_2–EP2 interactions in the cervix are unknown.

The objectives of the current investigation were to address the molecular mechanism of PGE_2 action in cervical stromal cells (CSCs) and the underlying pathways leading to cervical ripening. We hypothesized that PGE_2 would initiate specific cellular events in CSCs. Through physiological, genetic, and biochemical analyses on candidate human CSC (hCSC) genes, we report the downstream molecular mechanism by which PGE_2 down-regulates 15-PGDH in the human cervix. Our studies confirm that cervical ripening agents PGE_2 and misoprostol regulate metabolism of PGE_2 by transcriptionally inducing *COX-2* and *PTGES* and repressing *15-PGDH* via an EP2–histone deacetylase 4 (HDAC4)-dependent, feed-forward regulatory mechanism selective to hCSCs. Our studies further show that 15-PGDH is crucial for maintaining cervical competency during pregnancy in vivo and thus can be targeted by novel pharmacologic agents to induce cervical ripening and labor.

Results

PGE_2 Regulates the Transcriptome of hCSCs in Vitro Through EP2-Mediated Increases in Intracellular Ca^{2+}. RNA-sequencing (RNA-seq) data analysis and validation experiments identified PGE_2-mediated changes in the transcriptome of CSCs at both early (1 h) and late (24 h) time points. Interestingly, PGE_2 controlled its own metabolism by down-regulating the major PGE_2 catabolic enzyme 15-PGDH and up-regulating expression of two genes involved in PGE_2 synthesis (*COX-2* and *PTGES*) [Fig. 1 *A* and *B* and *SI Appendix*, Fig. S1; Gene Expression Omnibus (GEO) accession no. GSE99392]. Importantly, validation experiments confirmed that results obtained in CSCs from the nonpregnant cervix were relevant to those in cells from pregnant women at term (*SI Appendix*, Fig. S1). PGE_2 and misoprostol, but not $PGF_{2\alpha}$, sulprostone (EP3 agonist), or PGD_2, regulated *15-PGDH*, *PTGES*, and *COX-2* (Fig. 1*A*). These results are consistent with the prostanoid receptor expression profile in these cells in which EP2 receptors are highly expressed relative to other prostanoid receptors (Fig. 1*C*) and confirm that cervical ripening agents PGE_2 and misoprostol regulate metabolism of PGE_2 by activating *COX-2* and *PTGES* and repressing *15-PGDH* in a feed-forward regulatory mechanism. Three different EP2-selective antagonists (PF-04418948, TG4-155, and TG8-4) blocked PGE_2-mediated *15-PGDH* gene repression (Fig. 1*D*). Unlike classical PGE_2 signaling in other cells, PGE_2–EP2 interactions resulted in Ca^{2+}-dependent signaling (e.g., *DUSP1*, *c-fos*), not cAMP, PKA, and PI3-kinase (*SI Appendix*, Fig. S2).

Pathway analysis of the RNA-seq data indicated that the most significantly affected pathway by PGE_2 was Ca^{2+} signaling (Fig. 2*A*). Expression levels of 71 genes either regulated by Ca^{2+} or involved in Ca^{2+} signaling pathways were significantly changed [false discovery rate (FDR) < 0.05] by PGE_2 at either 1 or 24 h or both time points (Fig. 2*B*). Similar to PGE_2, treatment with Ca^{2+} ionophore (A23187) decreased 15-PGDH and increased COX-2 mRNA (Fig. 2*C* and *SI Appendix*, Fig. S3). Ca^{2+}-dependent PGE_2-mediated *15-PGDH* repression was confirmed using a cell-permeable intracellular Ca^{2+} chelator BAPTA-AM (Fig. 2*D*). Pretreatment with BAPTA-AM had little effect on PGE_2-mediated *15-PGDH* repression in growth medium containing Ca^{2+}. In Ca^{2+}-free medium, however, BAPTA-AM blocked PGE_2-mediated *15-PGDH* repression (Fig. 2*E*). Addition of Ca^{2+} to Ca^{2+}-free medium reversed this effect (Fig. 2*E*). Taken together, these results confirm that PGE_2-mediated down-regulation of *15-PGDH* is transduced through EP2 receptors and is Ca^{2+}-dependent in hCSCs.

PGE_2 Down-Regulates *15-PGDH* Gene Expression in Vitro by Increasing HDAC4. Because intracellular Ca^{2+} results in activation of HDACs (13) and HDAC inhibitors (HDACis) have been shown to induce *15-PGDH* gene expression in several mammalian cell types (14–16), we hypothesized that PGE_2-mediated Ca^{2+} signaling activates HDACs, which in turn regulate *15-PGDH*. ChIP results indicated that acetylated histone H3 levels associated with *15-PGDH* promoter decreased ∼fivefold in response to PGE_2 treatment (Fig. 3*A*). Immunoblotting indicated that three different nonselective HDACis increased 15-PGDH protein (Fig. 3*B*). As a positive control for HDACi action, acetylated histone H3 levels were probed, which also increased several fold in response to various HDACis (Fig. 3*B*). Further, treatment with three different HDACis increased mRNA levels of 15-PGDH significantly in a dose- and time-dependent manner (Fig. 3 *C* and *D*). Interestingly, HDACis induced 15-PGDH mRNA expression even in the presence of PGE_2 or A23187 (*SI Appendix*, Fig. S4), irrespective of order of treatment (delayed or primed). Thus, HDACs are mediators of PGE_2-induced *15-PGDH* gene repression.

To identify the specific HDAC involved in PGE_2-mediated regulation of *15-PGDH* in hCSCs, we first studied PGE_2-mediated changes in expression of various *HDAC* genes using our RNA-seq dataset. Among class I and II HDACs, *HDAC5* and *9* mRNA decreased in response to PGE_2 (Fig. 3*E*). In contrast, *HDAC4* mRNA increased ∼fourfold (Fig. 3*E*). Experiments confirmed that PGE_2 increased HDAC4 mRNA in a dose- and time-dependent manner, concomitantly decreasing *15-PGDH* in hCSCs (Fig. 4*A* and *SI Appendix*, Fig. S5*A*). Misoprostol and an EP2 receptor-selective agonist (butaprost) also increased *HDAC4* gene expression (*SI Appendix*, Fig. S5*B*), and EP2 receptor-selective antagonists blocked PGE_2-mediated activation of *HDAC4* expression (Fig. 4*B*). PGE_2 also increased protein levels of HDAC4, which was blocked by EP2 receptor antagonist PF-04418948 (Fig. 4*C* and *SI Appendix*, Fig. S6). In contrast with colorectal carcinomas in which marked increases in HDAC2 activity diminished levels of 15-PGDH (14), siRNA-mediated knockdown of *HDAC2* did not affect

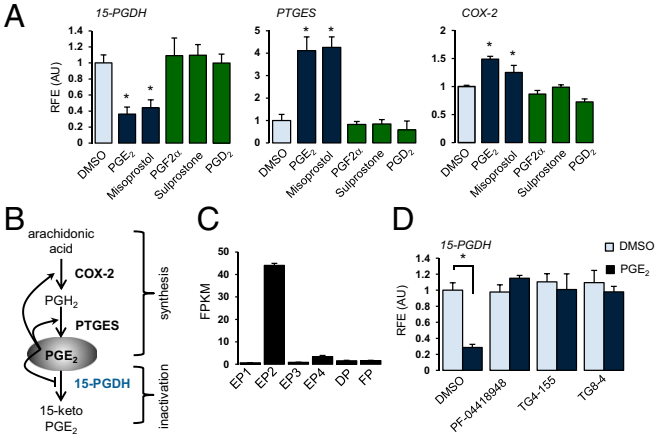

Fig. 1. PGE_2 regulates its own metabolism via EP2 receptors. (*A*) Relative mRNA levels of 15-PGDH (24 h), PTGES (24 h), and COX-2 (6 h) after treatment with DMSO or 100 nM of PGE_2, misoprostol, $PGF_{2\alpha}$, sulprostone, or PGD_2. (*B*) Feedback mechanism of PGE_2 metabolism. PGE_2 increases COX-2 and PTGES, simultaneously decreasing *15-PGDH*, thereby positively regulating its own metabolism. (*C*) Prostanoid receptor profile in hCSCs. Data represent fragments per kilobase of exon per million fragments mapped (FPKM) from RNA-seq datasets. (*D*) 15-PGDH mRNA levels in hCSCs pretreated with DMSO or EP2-selective antagonists (2 μM) for 1 h followed by treatment with either DMSO or PGE_2 (100 nM) for 24 h. (*A* and *D*) Data represent relative mean ± SD of triplicates normalized to GAPDH from at least three different cell preps. *$P < 0.05$ compared with DMSO treatment. RFE (AU), relative fold expression (arbitrary units).

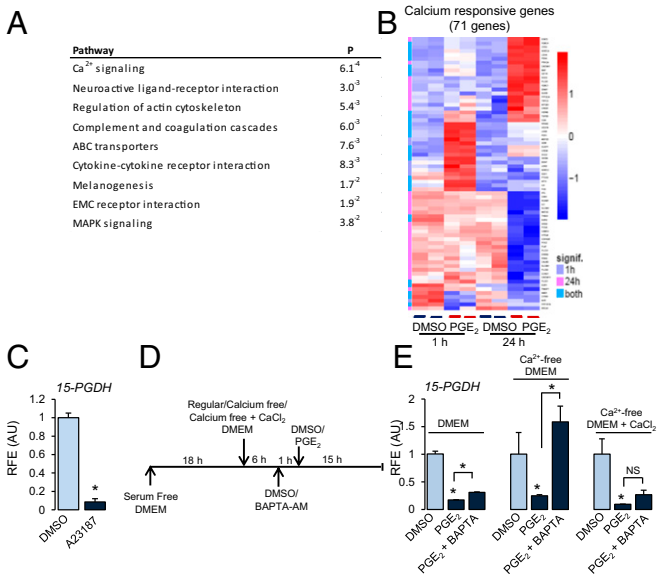

Fig. 2. PGE_2-mediated gene regulation is Ca^{2+}-dependent. (*A*) Pathway analysis of RNA-seq data (24 h). (*B*) Heatmap represents hierarchical clustering of known Ca^{2+} responsive genes and genes involved in calcium signaling differentially expressed (log-twofold change > 1.5) between control and PGE_2 at 1 and 24 h. (*C*) 15-PGDH mRNA in hCSCs after treatment with Ca^{2+} ionophore A23187 (10 nM) for 24 h. (*D* and *E*) Cells maintained in serum-free DMEM and then incubated in DMEM, Ca^{2+}-free DMEM, or Ca^{2+}-free medium + $CaCl_2$ (200 mg/L) for 6 h, pretreated with either DMSO or BAPTA-AM (1 μM) for 1 h. Thereafter, cells were treated with DMSO or PGE_2 (25 nM) for 15 h. Data represent 15-PGDH mRNA as mean ± SD of triplicates normalized to *GAPDH*. $^*P < 0.01$ compared with DMSO, ANOVA followed by Tukey's post hoc testing. RFE (AU), relative fold expression (arbitrary units).

15-PGDH gene expression in hCSCs (*SI Appendix*, Fig. S7*A*). Among class III HDACs (sirtuins), SIRT2 levels increased twofold within 1 h of treatment (*SI Appendix*, Fig. S7*B*), but unlike HDACis, the SIRT inhibitor, aristoforin, did not alter *15-PGDH* gene expression (*SI Appendix*, Fig. S7*C*).

To determine if Ca^{2+} is involved in PGE_2-mediated *HDAC4* gene expression, experiments were conducted as described in Fig. 2*D*. Whereas absence of extracellular Ca^{2+} alone was ineffective, chelation of intracellular Ca^{2+} by BAPTA-AM resulted in decreased HDAC4 mRNA (Fig. 4*D*). Further, pretreatment of hCSCs with BAPTA-AM completely blocked PGE_2-mediated increases in *HDAC4* gene expression in all conditions (Fig. 4*D*). Thus, in hCSCs, PGE_2 increases *HDAC4* gene expression via EP2 receptors, and *HDAC4* and *15-PGDH* genes are inversely regulated by PGE_2 in a Ca^{2+}-dependent manner. Interestingly, PGE_2 treatment did not change *HDAC4* gene expression in cell types with different EP receptor profiles [MCF7 (17) and MEL5 (18); *SI Appendix*, Fig. S8].

Next, the crucial role of HDAC4 in mediating 15-PGDH gene expression in hCSCs was established. Specifically, siRNA-mediated knockdown of *HDAC4* increased, whereas adenovirus-mediated overexpression decreased basal levels of 15-PGDH mRNA, suggesting that *15-PGDH* is an HDAC4 target gene (Fig. 4*E* and *SI Appendix*, Fig. S9). Notably, knockdown of *HDAC4* abrogated PGE_2-mediated down-regulation of *15-PGDH* gene expression (Fig. 4*E*), suggesting that HDAC4 is necessary to mediate down-regulation of this gene. The opposing actions of HDAC4 siRNA and PGE_2 resulted in no change in *HDAC4* expression levels (Fig. 4*E*). These findings are compatible, therefore, with the lack of dramatic *HDAC4* knockdown effects on PGE_2-mediated down-regulation of *15-PGDH* (Fig. 4*E*). LMK-235 (an HDAC4/5 selective enzyme inhibitor) treatment resulted in five- to sixfold increases in basal levels of 15-PGDH mRNA and protein (Fig. 4*F*). LMK-235 also blocked PGE_2-mediated down-regulation of *15-PGDH* gene expression (Fig. 4*F*). However, siRNA-mediated knockdown of *HDAC5* did not alter *15-PGDH* gene expression in these cells, indicating that the effects of LMK-235 are mediated through inhibition of HDAC4, not HDAC5 (*SI Appendix*, Fig. S10). Interestingly, siRNA-mediated knockdown of *HDAC4* together with LMK-235 treatment led to cumulative loss of HDAC4 mRNA and synergistic activation of *15-PGDH* gene expression (Fig. 4 *G* and *H*). Collectively, results indicate that PGE_2-mediated increases in HDAC4 expression and its deacetylase activity are crucial for PGE_2-mediated down-regulation of *15-PGDH* in hCSCs.

PGE_2 Mediates HDAC4 Nuclear Import in Vitro. Immunofluorescence studies show weak HDAC4 immunostaining distributed in both cytoplasmic and nuclear compartments in baseline hCSCs treated with vehicle (Fig. 5 *A* and *B*). Treatment with PGE_2 resulted in not only an overall increase in HDAC4 immunofluorescence but also increased nuclear localization (Fig. 5 *A* and *B*). Immunoblotting clearly shows that nuclear HDAC4 levels increased within 1 min of treatment with PGE_2 and steadily increased as a function of time (Fig. 5 *C* and *D*). Cytoplasmic HDAC4 levels did not change until

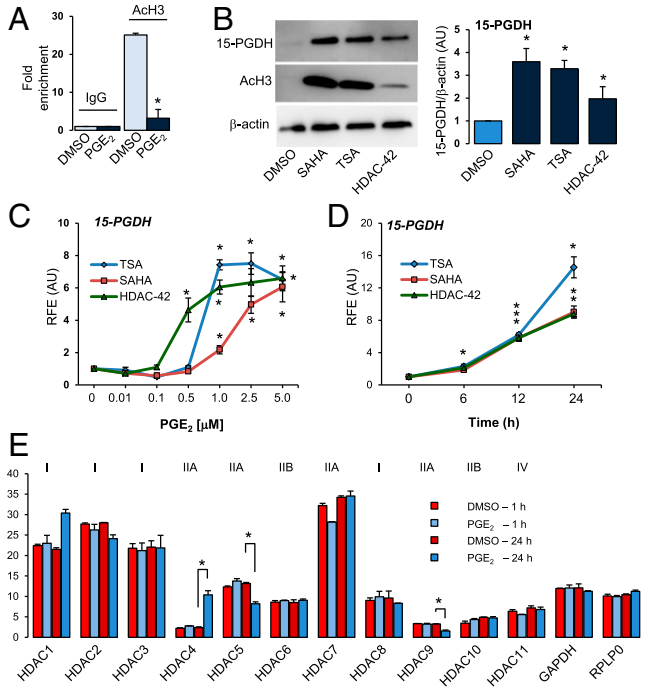

Fig. 3. PGE_2 results in deacetylation of chromatin associated with the 15-PGDH gene promoter. (*A*) Chromatin immunoprecipitation (IP) of acetylated histone H3 (AcH3) is compared with IP of IgG (negative control) in cells treated with DMSO or PGE_2 (100 nM) for 24 h. Data represent average fold enrichment. $^*P < 0.05$ compared with DMSO, Student's *t* test. $n = 3$. (*B*) Representative immunoblot and quantitation of 15-PGDH levels in hCSCs treated with DMSO or HDACi SAHA (2.5 μM), TSA (1 μM), or HDAC-42 (1 μM) for 24 h. Acetylated histone H3(AcH3), positive control; β-actin, loading control. $^*P < 0.05$ compared with DMSO, Student's *t* test. $n = 3$. (*C*) Dose- (24 h) and time-dependent [SAHA (2.5 μM), TSA (1 μM), or HDAC-42 (1 μM)] increases in *15-PGDH* after treatment with HDACi. $^*P < 0.05$ compared with DMSO (*C*) or 0 time point (*D*), ANOVA, Dunn's post hoc testing. $n = 3$. (*E*) Data represent fragments per kilobase of exon per million fragments mapped (FPKM) of class I, IIA, IIB, and IV HDACs expressed in hCSCs treated with DMSO or PGE_2 (100 nM) for 1 or 24 h mined from the RNA-seq dataset. GAPDH and RPLP0 are shown as controls (1/100th FPKM values). $^*P < 0.05$ compared with corresponding DMSO control.

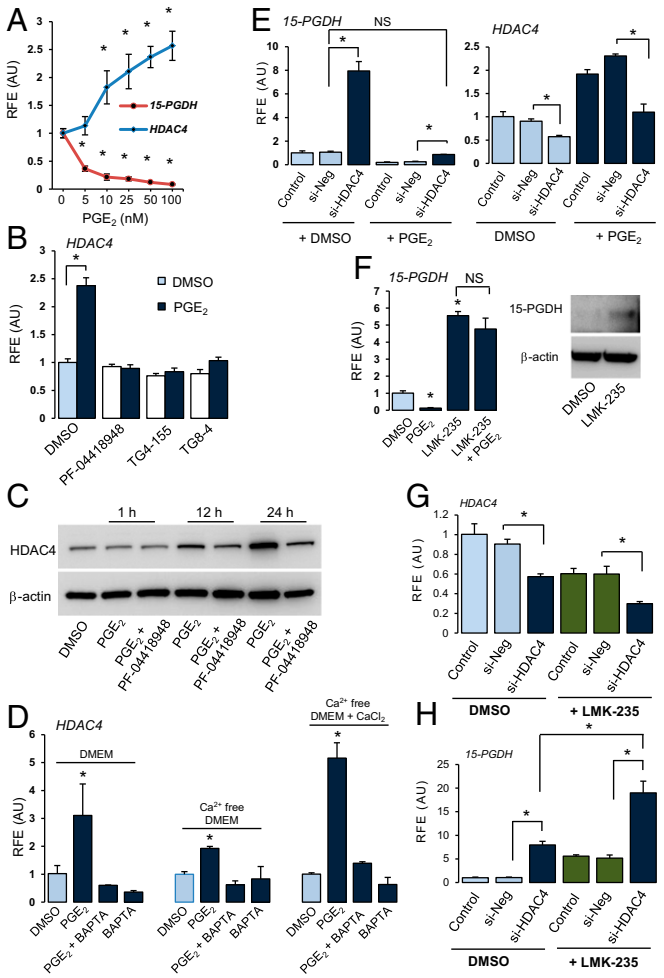

Fig. 4. PGE_2-mediated 15-PGDH repression is mediated by HDAC4. (*A*) HDAC4 and 15-PGDH mRNA after treatment with increasing concentrations of PGE_2 for 24 h. (*B*) HDAC4 mRNA in hCSCs pretreated with DMSO or EP2-selective antagonists (2 μM) for 1 h followed by either DMSO or PGE_2 (100 nM) for 24 h. (*C*) HDAC4 protein levels in hCSCs pretreated with DMSO or PF-04418948 (2 μM) followed by DMSO or PGE_2. β-actin, loading control. (*D*) *HDAC4* in hCSCs in media ± Ca^{2+}, pretreated with DMSO or BAPTA-AM (1 μM) for 1 h, then with DMSO or PGE_2 (25 nM) for 15 h. (*E*) *15-PGDH* and *HDAC4* expression levels after siRNA-mediated knockdown with control negative siRNA or siHDAC4 for 48 h followed by treatment with DMSO or PGE_2 (100 nM) for 24 h. (*F*) 15-PGDH mRNA quantified in hCSCs treated with DMSO or PGE_2 (25 nM) in combination with LMK235 (500 nM). Immunoblot of 15-PGDH protein levels in whole-cell protein extracts prepared from hCSCs treated with DMSO or LMK-235 (1 μM) for 24 h. β-actin, gel loading control. (*G* and *H*) HDAC4 (*G*) and 15-PGDH (*H*) mRNA levels in hCSCs transfected with no siRNA, control siNeg, or si-HDAC4 with or without the HDAC4/5 enzyme inhibitor LMK-235. Bars represent relative mean ± SD of triplicates. *$P < 0.01$, ANOVA followed by Dunnett's test using vehicle or DMSO/si-Neg as control. Experiment was repeated in three cell preps with identical results.

6 h after treatment, after which levels increased and remained elevated (Fig. 5 *C* and *D*). These changes in nuclear localization of HDAC4 were accompanied by changes in the phosphorylation status of HDAC4 (Fig. 5 *E* and *F*). HDAC4 (Ser246) was dephosphorylated in response to PGE_2 treatment within 1 h. Total HDAC4 protein levels did not change during this time period but increased at later times (Fig. 5 *E* and *F*). Although immunoblotting of phospho-HDAC4 alone indicates that HDAC4 phosphorylation seems to recover at later time points, normalization to increased protein levels of HDAC4 indicates that phosphorylation of HDAC4 actually decreased with time (Fig. 5*F*). In sum, PGE_2 induces HDAC4 dephosphorylation and nuclear relocalization.

Phosphorylation of class II HDACs by serine/threonine kinases regulates their cellular localization, stability, and ability to regulate targeted gene expression (19, 20). Phosphorylated HDAC4 binds 14-3-3 protein, a complex retained in the cytoplasm (21). Dephosphorylation of cytoplasmic HDAC4, on the other hand, leads to release from the complex and nuclear import of HDAC4 (22). Nuclear Ca^{2+}/calmodulin-dependent protein kinase II (CaMKII) binds and phosphorylates nuclear HDAC4 for export to the cytoplasm (23). CaMKII inhibitors KN62 and KN93 down-regulated *15-PGDH* 40–60% mimicking PGE_2 (*SI Appendix*, Fig. S11*A*). As expected, inhibition of CaMKII did not affect *HDAC4* gene expression (*SI Appendix*, Fig. S11*A*). Likewise, treatment with a cytosolic serine/threonine phosphatase activator C2 ceramide (24) repressed *15-PGDH* but with no effect on *HDAC4* (*SI Appendix*, Fig. S11*B*). Further treatment with okadaic acid, which was previously shown to block HDAC4 de-phosphorylation by inhibiting protein phosphatase 2A (22), prevented PGE_2-mediated down-regulation of *15-PGDH* (*SI Appendix*, Fig. S11*C*). Okadaic acid, however, did not alter KN-93–mediated down-regulation of *15-PGDH* gene expression (*SI Appendix*, Fig. S11*D*). These results, therefore, are compatible with the overall pathway in which PGE_2 signaling regulates not only expression of *HDAC4* but also HDAC4 cellular localization, thereby bringing about targeted repression of *15-PGDH* (Fig. 5*D*).

HDAC4 Levels and Localization During Late Gestation in Human Cervical Stromal Tissues in Vivo. To determine if *HDAC4* expression is regulated in human cervical stromal tissues during the course of cervical ripening, relative levels of HDAC4 mRNA and protein localization were determined in human cervical stromal tissues from nonpregnant and pregnant women (*SI Appendix*, Table S1). HDAC4 mRNA levels were increased significantly in stroma from pregnant women in late gestation (35–42 wk) compared with those from nonpregnant or pregnant women in early gestation (Fig. 6*A*). mRNA levels for 15-PGDH were decreased significantly in stroma of women in labor compared with nonpregnant or stromal tissues before cervical ripening (Fig. 6*A*). Immunostaining indicated that HDAC4 was present in the cytoplasm of some, but not all, cervical stromal fibroblasts from nonpregnant women (Fig. 6 *B*, *a*). Before cervical ripening in late pregnancy, HDAC4 immunoreactivity was abundant in most CSCs and localized to the cytoplasm (Fig. 6 *B*, *b*). In the ripe cervix at term, HDAC4 immunoreactivity was present in virtually all CSCs and distributed in both cytoplasmic and nuclear compartments (Fig. 6 *B*, *c*). In contrast with the unripe cervix, HDAC4 protein staining was intense and predominantly localized in the nucleus during cervical dilation in labor (Fig. 6 *B*, *d*).

Down-Regulation of *15-PGDH* Is Crucial for PGE_2-Induced Preterm Labor in Mice. A precisely timed pregnant mouse model was used to determine the importance of PGE_2-mediated regulation of *15-PGDH* for cervical ripening and labor. I.p. injection of pregnant mice with PGE_2 did not alter duration of gestation, with all mice delivering at the expected time on d 19 dpc (days post coitum) similar to vehicle-treated animals (Fig. 7*A*). We reasoned that high levels of 15-PGDH enzyme and rapid inactivation of PGE_2 lead to failure of PGE_2 to induce preterm labor. Interestingly, treatment with metabolism-resistant 16,16,-dimethyl PGE_2 ($dmPGE_2$) that also induced *HDAC4* and decreased *15-PGDH* mRNA levels in hCSCs (*SI Appendix*, Fig. S12*A*) caused preterm birth on d 15 within 8–12 h. All pups were dead at the time of delivery, with evidence of mechanical trauma. Sacrifice of pregnant animals 6 h after $dmPGE_2$ treatment on d 15 revealed a tonically contracted uterus, intrauterine death, and pallid pups consistent with lack of oxygenation (*SI Appendix*,

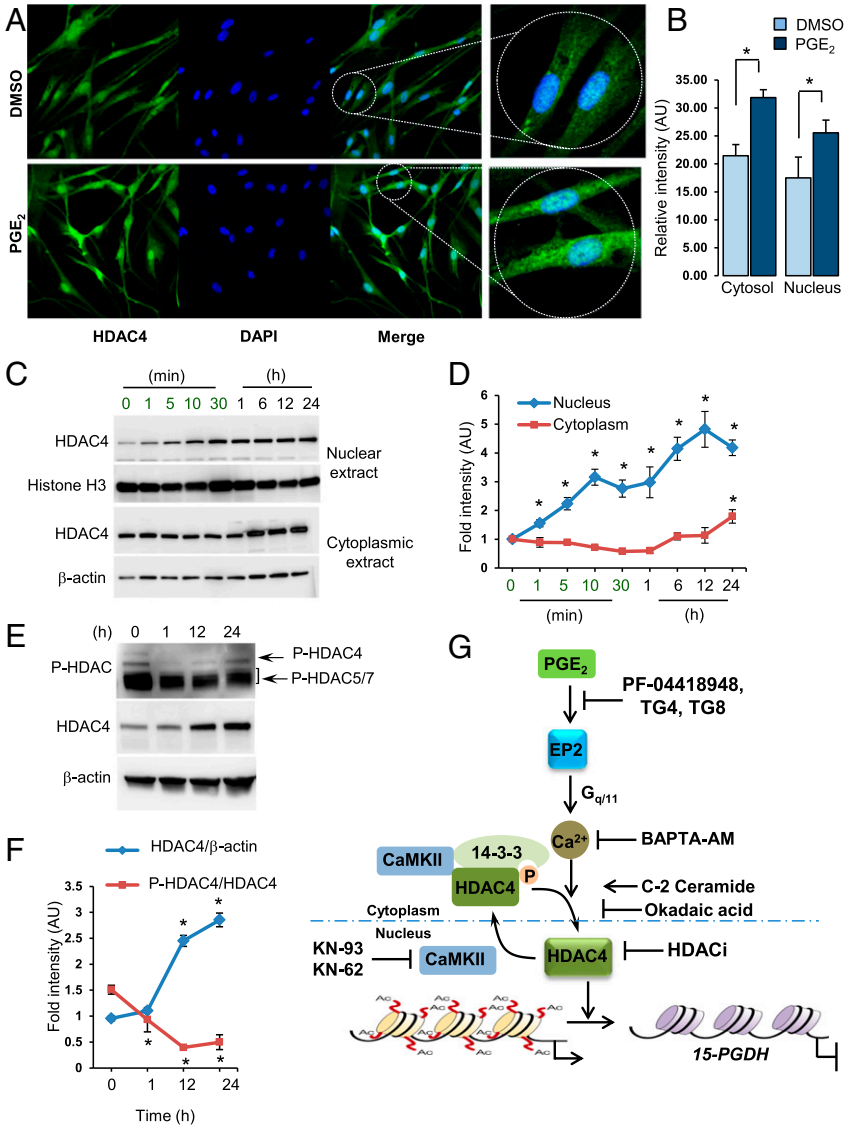

Fig. 5. PGE_2-mediated dephosphorylation of HDAC4 and nuclear localization. (*A*) Immunocytostaining of hCSCs with HDAC4 antibody after treatment with DMSO or PGE_2 (100 nM) for 24 h. Microscopic images were captured using 63× objective under similar settings. (*B*) Data represent relative fluorescent signal intensity ± SEM, quantified from confocal images. *$P < 0.05$ compared with DMSO, Student's *t* test. (*C* and *D*) Representative immunoblot and quantitation of HDAC4 protein in nuclear and cytoplasmic fractions of hCSCs treated with PGE_2 (100 nM) for indicated times. Histone H3 and β-actin, gel loading controls. *$P <$ 0.05 compared with DMSO, Student's *t* test. $n = 3$. (*E* and *F*) Phosphorylation profile of HDAC4 (Ser246) and HDAC4 protein levels in response to PGE_2 treatment in hCSCs as a function of time. β-actin, gel loading control. *$P < 0.05$ compared with DMSO, Student's *t* test. $n = 3$. (*G*) PGE_2 acts through EP2 receptors to increase Ca^{2+}-dependent dephosphorylation of cytoplasmic HDAC4. Dephosphorylation of HDAC4 relieves binding to its cytoplasmic chaperone 14-3-3, resulting in nuclear translocation and deacetylation of chromatin associated with the 15-PGDH gene promoter. Nuclear CaMKII restores nuclear HDAC4 levels by phosphorylation and export to the cytoplasm. EP2 receptor antagonists and HDACis prevent PGE_2-mediated *15-PGDH* gene repression.

Fig. S12*B*). Because $dmPGE_2$ is a competitive inhibitor of 15-PGDH, we sought to determine if inhibition of 15-PGDH led to cervical ripening and preterm birth. However, treatment with a 15-PGDH inhibitor, SW033291 (25), alone did not affect gestational length, and offspring were born healthy and full-term (Fig. 7*A*). Interestingly, treatment with a combination of PGE_2 and SW033291 induced preterm labor within 12–48 h in 100% of animals (Fig. 7*A*). Combination treatment did not cause fetal death in utero and premature pups born on d 15 or d 16 delivered atraumatically with intact placentas and fetal membranes (Fig. 7*B*). Premature pups born on late d 16 or d 17 were alive but died shortly thereafter due to extreme prematurity (Fig. 7*C*). Perhaps the most interesting aspect of this treatment (PGE_2 + SW033291) is that mice delivered only two pups closest to the cervix, whereas the remaining pups were retained, delivering at the expected time on day 19 alive and healthy, suggesting that the predominant effect of PGE_2 + 15-PGDH inhibitor was on the cervix and lower uterine horns (Fig. 7*D*). Thus, we assessed the impact of treatment on histomorphology of the cervix. In vehicle-treated animals, the endocervix was lined by a layer of 4–5 pseudostratified columnar epithelial cells that progressively differentiate from the basal epithelium to fully developed mucus-secreting cells toward the lumen (Fig. 7*E*). The collagenous stromal matrix was dense and well-organized. Epithelial and stromal morphology was similar in vehicle-, PGE_2-, or SW033291 alone-treated animals (Fig. 7*E*). In contrast, treatment with PGE_2 + SW033291 resulted in increased size and numbers of mucus-laden epithelial cells and dramatic remodeling

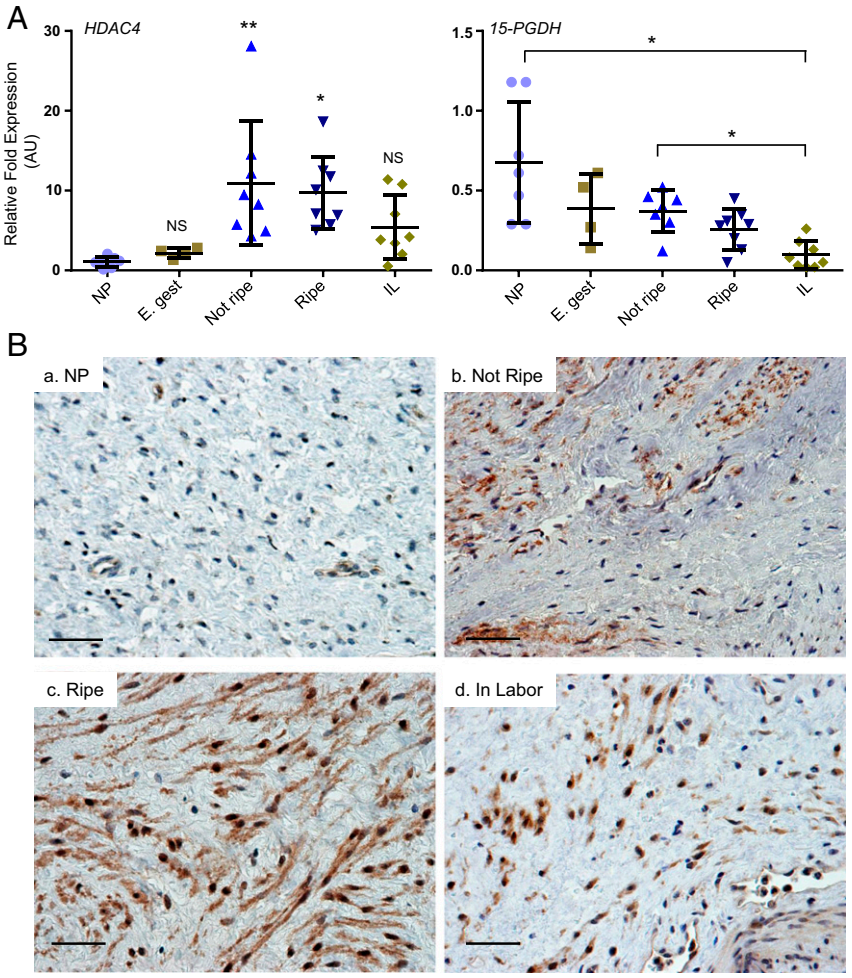

Fig. 6. HDAC4 mRNA and protein levels in human cervical stromal tissues at different stages of pregnancy. (*A*) HDAC4 and 15-PGDH mRNA levels quantified in human cervical stromal tissues obtained from nonpregnant (NP, $n = 7$), pregnant early gestation (E. gest, $n = 4$), pregnant with cervix not ripe and not in labor (near term, Not Ripe, $n = 7$), term pregnant with cervix ripe before labor (Ripe, $n = 8$), and term pregnant in labor (IL, $n = 7$). Data represent relative mRNA levels normalized to GAPDH mRNA levels. $^*P < 0.05$, $^{**}P < 0.001$ compared to nonpregnant. NS, not significant. ANOVA followed by Tukey's multiple comparisons test. AU, arbitrary unit. (*B*) Immunolocalization of HDAC4 in human cervical stroma of (*a*) nonpregnant (NP) and (*b*) pregnant women in early gestation (10–14 wk), at term before cervical ripening (Not Ripe), (*c*) term after cervical ripening but before labor (Ripe), and (*d*) in labor (In Labor). Results were consistent, representing 3–4 tissues in each group. (Scale bar, 20 μm.)

of the collagenous matrix surrounding the stromal fibroblasts and smooth muscle cells (Fig. 7*E*). Biomechanical properties of cervices (on d 16) from treated animals were determined. Although similar in PGE_2- and SW033291-treated animals, baseline cervical dilation was increased in combination-treated animals compared with controls (Fig. 7*F*). This increase in baseline dilation was accompanied by significant increases in distensibility without compromise of maximal force (Fig. 7*F*). The results, together with the preterm delivery phenotype, indicate that 15-PGDH plays a crucial role in maintenance of cervical competency during pregnancy in the presence of increasing levels of PGE_2 and that down-regulation of cervical *15-PGDH* is a prerequisite for PGE_2 action at term for delivery.

Discussion

Studies reported here used CSCs in culture to elucidate the molecular pathways of PGE_2 action in the human cervix. Human cervical tissues confirmed differential regulation of HDAC4 localization during human cervical ripening. Finally, studies in the mouse indicate that down-regulation of 15-PGDH is a crucial component of successful PGE_2-induced cervical ripening and labor. The experiments suggest that continuous doses of $PGE_{2/1}$ may fail to induce cervical ripening and labor if endogenous levels of cervical 15-PGDH are high. Therefore, 15-PGDH represents an enzyme important for cervical competency during pregnancy.

It is well-known that COX-2-derived PGE_2 plays a major role in cervical ripening during term and preterm birth (7, 11, 26–28). Inhibition of COX-2 during pregnancy, however, is relatively contraindicated because PGE_2 interacting with EP4 receptors is crucial for patency of the fetal ductus arteriosus (29, 30). The studies reported herein indicate that EP2, not EP4, receptors mediate the effects of PGE_2 in CSCs. Activation of EP2 receptors led to decreased expression of *15-PGDH* through detailed intracellular events unique from EP2 signaling in other cells. Specifically, activation of stromal cell EP2 receptors led to increases in intracellular Ca^{2+}, Ca^{2+}-dependent dephosphorylation of cytoplasmic HDAC4, which is then localized to the nucleus to modify the transcriptome of hCSCs. Further, we show that PGE_2-mediated down-regulation of its own catabolic enzyme, 15-PGDH, was required for PGE_2-mediated cervical ripening.

RNA-seq data confirmed that PGE_2 activates Ca^{2+} signaling pathways in hCSCs. Early cellular events after EP2 activation included Ca^{2+}-dependent dephosphorylation of HDAC4 and its nuclear import. Phosphorylation of class II HDACs by serine/threonine kinases regulates their cellular localization, stability, and

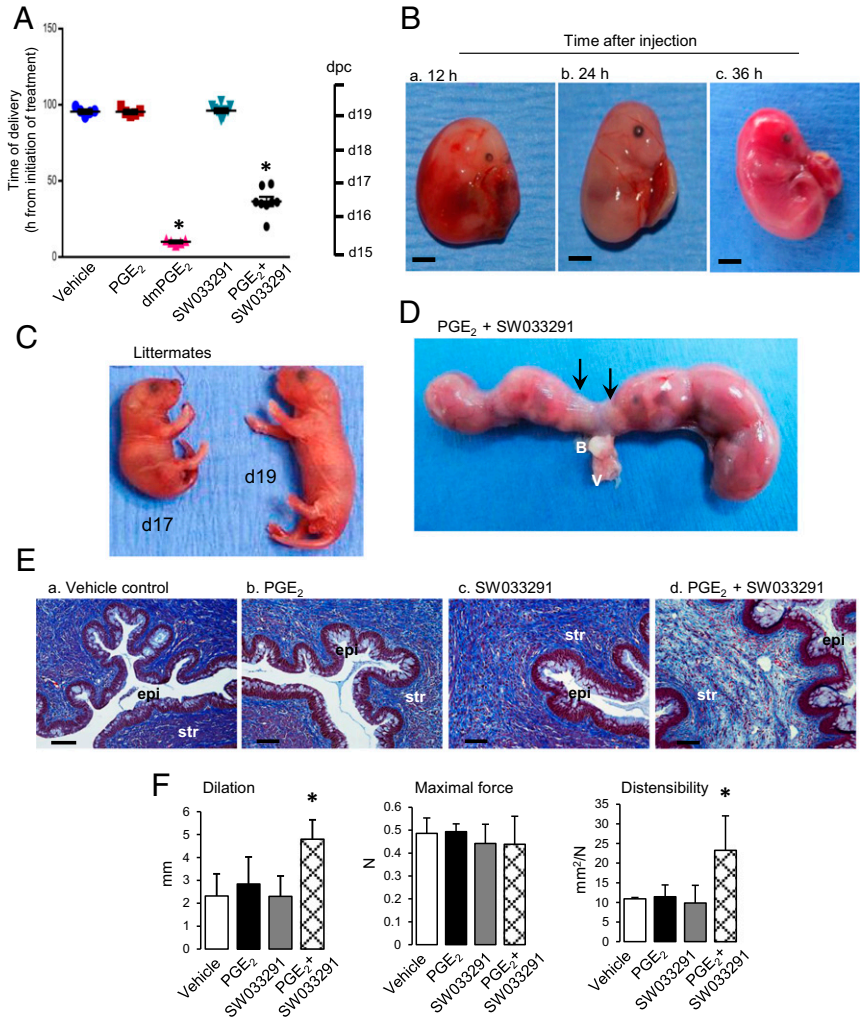

Fig. 7. PGE_2 plus 15-PGDH inhibitor treatment induces preterm cervical ripening and labor in mice. (*A*) Time (h) of delivery from the initiation of different treatments as indicated. Gestation day (days post coitum, dpc) are shown on *Right*. *$P < 0.01$ ANOVA with Tukey's post hoc testing. (*B*) Preterm pups born born intact with fetal membranes and placenta 12 h (*a*), 24 h (*b*), or 36 h (*c*) after treatment with PGE_2 + SW033291. (Scale bar, 2.5 mm.) (*C*) PGE_2 + SW033291-induced delivery of littermates born on d 17 (*Left*) and early d 19 (*Right*). (*D*) Female reproductive tract dissected on d 17 for assessment of fetal health and gross morphological changes in cervix and uterus. Arrows indicate delivery of cervical pups in animals treated with PGE_2 + SW033291. B, bladder; V, vagina. (*E*) Masson's trichrome stain of midcervical transverse sections of mice treated with (*a*) vehicle, (*b*) PGE_2, (*c*) SW033291, or (*d*) PGE_2 + SW033291. Animals were treated bidaily on d 15 and d 16 with tissue collection on late d 16 before delivery. (Bar, 200 μm.) epi, epithelium; str, stroma. (*F*) Baseline dilation, maximal force generation, and distensibility of cervices from animals treated with vehicle ($n = 3$), PGE_2 ($n = 5$), SW033291 ($n = 5$), or PGE_2 + SW033291 ($n = 5$). Data represent mean ± SEM. *$P < 0.01$ ANOVA with Tukey's post hoc testing.

ability to regulate targeted gene expression (19, 20). Phosphorylated HDAC4 binds 14-3-3 protein, a complex retained in the cytoplasm (21). Dephosphorylation of cytoplasmic HDAC4 by protein phosphatase 2A, on the other hand, leads to release from the complex and nuclear import of HDAC4 (22). Global inhibition of serine/threonine phosphatases with okadaic acid confirmed that dephosphorylation of HDAC4 was an important signaling event. After the initial dephosphorylation of HDAC4 and changes in gene expression (including *cfos*), HDAC4 increased as a function of time, and *DUSP1* mRNA remained increased for up to 24 h. These findings suggest that EP2 signaling results in an early increase in intracellular Ca^{2+} and dephosphorylation of HDAC4 but that later events continue to promote the signals. Recently, it was shown that electrical stimulation of cervix leads to cervical softening and labor in rats (31). Because electrical stimulation results in depolarization of the cell membrane and influx of Ca^{2+}, we suggest that electrical stimulation of the cervix stimulates increases in intracellular Ca^{2+} and downstream effects of PGE_2 including dephosphorylation of HDAC4 and suppression of *15-PGDH*. Further, in the presence of an intact capillary bed with extracellular Ca^{2+}, the resulting increase in $[Ca^{2+}]_i$ is likely to activate phospholipases, release arachidonic acid, and thereby amplify the feed-forward effects of COX-2 activation on the cervix.

The role of 15-PGDH in preterm birth has been studied previously (32). The 15-PGDH hypomorphic mice with low levels of 15-PGDH delivered almost 24 h early, but pups were required to be hypomorphic for this effect on gestational length (32). In keeping with this observation, in our mouse model, inhibition of 15-PGDH alone did not alter gestational length. Treatment of pregnant mice with a combination of PGE_2 and 15-PGDH inhibitor SW033291 induced preterm cervical ripening and labor in all animals tested. More provocative is that delivery was always incomplete. Pups from the ovarian end of each horn were retained and delivered at term on d 19 with normal growth and development. Maintenance of pups at the ovarian ends suggests that this ripening was not accompanied by strong uterine contractions or progesterone withdrawal in which the uterus empties completely.

Interestingly, RNA-seq data did not reveal PGE_2-mediated increased expression of proteases (or down-regulation of protease inhibitors), hyaluronan synthases, or progesterone receptors. Further, although PGE_2 suppressed collagen type VI gene expression, the predominant fibrillar collagens were not affected. Decreases in COLA6A as well as differential regulation of integrin receptors may alter the matrix environment and matricellular signaling in the cervix. An important consideration, however, is PGE_2-mediated increases in genes involved in cytokine–cytokine receptor interactions (e.g., *CCL8*, *CXCL-1* and *-2*, *IL1R1*, and several members of the TNF/TNF receptor superfamily), suggesting that PGE_2 may alter matrix remodeling of the cervix indirectly through stromal cell recruitment and activation of immune cell types within the cervix. Nonetheless, the key finding is the crucial role of 15-PGDH in regulating all aspects of PGE_2 action in the cervix.

This investigation identifies (*i*) EP2 receptor antagonists, (*ii*) HDACis, and (*iii*) activators of 15-PGDH as potential interventions to prevent preterm shortening of the cervix and preterm birth. With the discovery of several biologically active EP2 selective antagonists in the last 4 y, these can be considered as potential safer alternatives for COX-2 inhibitors in pregnant women with preterm shortening of the cervix or risk for preterm birth. Although differences in EP receptor profiles in the cervix of rats and mice compared with humans do not allow us to test EP2-selective antagonists in animals, the potential for these therapeutic targets to impact initiation, propagation, and rate of cervical ripening in pregnant women is supported by (*i*) down-regulation of *15-PGDH* in cervical stromal tissues of pregnant women during cervical ripening (6), (*ii*) EP2 receptor predominance in cervical tissues obtained from pregnant women, (*iii*) increased HDAC4 mRNA in the pregnancy cervix, and (*iv*) progressive increases in nuclear localization of HDAC4 in stromal cells of the cervix from before ripening, during ripening before labor, to the dilated ripe cervix in labor. Further, we confirmed previous studies in which the HDACi TSA delayed parturition in mice (33) and found that extension of treatment time delayed parturition for up to 3 d without immediate adverse effects on the fetus. Taken together with our in vitro data, we suggest that HDACis target HDAC4 to increase basal levels of 15-PGDH that neutralizes active PGE_2 and $PGF_{2\alpha}$. With many HDACi considered as therapeutics for various diseases and well-established pharmacokinetics and toxicity profiles, identification of HDAC4 as a key regulatory intermediate for PGE_2 action on the cervix may lead to new strategies to inhibit, or prevent, preterm cervical ripening and preterm birth.

In summary, unraveling the signal transduction pathways of PGE_2 signaling in the cervix and identification of the crucial role of 15-PGDH in maintenance of cervical competency are important steps in understanding regulation of cervical function during pregnancy. We propose that 15-PGDH inhibitors with a short half-life and safe pharmacological profile may not only increase the success of PGE_2-induced cervical ripening but also facilitate use of lower doses of $PGE_{2/1}$ and thereby decrease the induction-to-delivery interval, an important consideration if induction of labor is conducted in an adverse perinatal environment. In contrast, development of EP2 antagonists and HDAC4 inhibitors may successfully interrupt the vicious cycle of preterm cervical ripening and preterm birth.

Materials and Methods

Cell Culture and Treatments. hCSCs were cultured as described previously. Briefly, all experiments in CSCs were conducted in cells obtained from nonpregnant women undergoing hysterectomy for benign gynecological conditions with one exception. The one exception was that CSCs from pregnant women undergoing cesarean-hysterectomy for placenta previa at term before the onset of labor were used to validate RNA-seq data. Dissected stromal tissues (from internal os to midcervix) were separated from the epithelium, washed with DMEM, and minced into tiny pieces followed by incubation in DMEM supplemented with 10% FBS for 18–20 d until cells grew onto the culture plates (passage 0). Cells were then trypsinized, subcultured once (passage 1), and used for various treatments. Cells were incubated in serum-free media for 24 h before treatments to completely remove FBS-derived prostanoids. PGE_2, $PGF2\alpha$, PGD_2, butaprost, misoprostol, sulprostone, PF-04418948, 8-bromo-cAMP, Wortmannin, A23187, TSA, SAHA, HDAC-42, KN-62, KN-93, C2-ceramide, okadaic acid, and 16,16-dimethyl PGE_2 were obtained from Cayman Chemical. Ly294002 and Aristoforin were obtained from Santa Cruz Biotechnology. BAPTA-AM was from ThermoFisher Scientific. LMK-235 was from Selleck Chemicals. TG4-155 and TG8-4 were synthesized as described previously (34). All reagents unless mentioned were dissolved in dimethyl sulfoxide (DMSO) and further diluted in DMSO for treatment of cells. Final concentration of DMSO was <0.2% for all treatments. All experiments were conducted in triplicates in at least three cell culture preparations from cervices obtained from different subjects.

Human Cervical Tissues. Cervical stromal tissues were obtained from nonpregnant women as described above and from pregnant women undergoing cesarean hysterectomy according to protocols approved by the Institutional Review Board at the University of Texas Southwestern Medical Center. Gestational age and other details were recorded, and cervical ripening was ascertained using a modified Bishop's score in pregnant women (35). In cases that precluded a clinical examination (i.e., placenta previa), cervical length was substituted for effacement (≥4 cm = 0, 2–3 cm = 1, and 0–2 cm = 2), station was presumed to be 0, and dilation of hysterectomy specimen was used to categorize cervical ripening. Cervical stroma was separated from endocervical epithelium from the internal os to midcervix. Ectocervix was not included. Clinical characteristics of pregnant women from whom samples were obtained are shown in *SI Appendix*, Table S1. Only the stromal region of the cervix was dissected and stored in RNA later for RNA extraction. Specimens were without contamination from cervical epithelium as determined by absent expression of epithelial 17βHSD2 (36). Another small section of cervix from the midcervix was formalin-fixed immediately and processed for immunostaining. Tissues from women with infections, trophoblast invasion into the cervix, cervical dysplasia, or steroid treatment were excluded.

RNA-Seq and Analysis. Total RNA samples were processed with the TruSeq Stranded Total RNA LT Sample Prep Kit from Illumina. Total RNA was isolated from two biological replicates of hCSCs treated with vehicle or PGE_2 for 1 or 24 h and processed for whole-genome polyadenylated RNA sequencing ($polyA^+$ RNA-seq). Total RNA samples were subjected to enrichment of $polyA^+$ RNA using Dynabeads Oligo(dT)25 (Invitrogen). Thereafter, strand-specific RNA-seq libraries were prepared as described previously (37) and sequenced using an Illumina HiSEq. **2500** using SBS v3 reagents for 100-bp paired-end reads. Reads were trimmed to remove adaptor sequences and low-quality bases using fastq-mcf (v1.1.2–806, https://github.com/ExpressionAnalysis/ea-utils/blob/wiki/FastqMcf.md), followed by mapping to human genome (hg19) using Tophat (v2.0.10, ref. 38) with igenome annotations (https://ccb.jhu.edu/software/tophat/igenomes.shtml). Duplicate reads were marked but not removed. FeatureCounts (39) was used for read counting and edgeR (40) for expression abundance estimation and differential expression test. Pathways enriched in differentially expressed genes were identified by DAVID (41, 42). RNA-seq datasets generated for this study are available at https://www.ncbi.nlm.nih.gov/geo/query/acc.cgi?acc=GSE99392.

RNA Extraction and qRT-PCR. RNA extraction from cells was performed using RNA extraction kit from Invitrogen (AM1914). RNA extraction from human cervical stromal tissues (*SI Appendix*, Table S1) was performed using guanidine hydrochloride extraction method as described elsewhere (43). cDNA synthesis was performed using iScript Reverse Transcription Supermix from BIO-RAD according to the supplier's protocol (170-8841). PCR was done using iTaq SYBR Green PCR Master mix (4309155) or TaqMan Gene expression master mix (4369016) from Applied Biosystems in an ABI 7900HT Fast Real-Time PCR system. Gene-specific oligonucleotide sequences and catalog numbers used for qRT-PCR are supplied in *SI Appendix*, Table S2.

Protein Extraction and Immunoblotting. Posttreatment cells were washed with cold PBS twice and scraped into RIPA buffer (50 mM Tris•HCl, 150 mM NaCl, 0.1% SDS, 0.5% sodium deoxycholate, 1% Nonidet P-40, protease inhibitor mixture), vortexed for 30 s, and incubated on ice for 30 min. Lysates were then centrifuged at 9,300 × *g* for 5 min at 4 °C. Clear supernatants were collected and protein amounts were quantified using BCA protein assay kit from ThermoScientific (23223, 23224). Cytoplasmic and nuclear protein fractions were prepared as described previously (44). We resolved 40 μg of whole cell/cytoplasmic or 20 μg of nuclear protein extracts using Mini-PROTEAN

TGX gels from BIO-RAD (456-9033) and transferred them to PVDF membrane (BIO-RAD, 162–0177). Membranes were blocked with 5% skim milk solution in TBS for 1 h at room temperature followed by incubation with specific antibodies against 15-PGDH (Cayman Chemical, 1606 15), HDAC4 (Cell Signaling, 7628), phospho-HDAC4(Ser246)/HDAC5 (Ser259)/HDAC7(Ser155) (Cell Signaling, 3443), acetylated histone H3 (Millipore, 06–599), or β-actin (Cell Signaling, 4967) overnight at 4 °C. Blots were then washed with PBS containing 0.1% Tween 20 and further incubated with HRP-conjugated secondary antibodies (anti-rabbit 170–6515 or anti-mouse 170–6516; BIO-RAD) followed by washing and developed using SuperSignal West Pico chemiluminescent kit (Thermo Scientific, 34080). Immunospecific signals were detected using FujiFilm LAS-3000 imager. For reprobing with different antibodies, membranes were stripped using One-Minute Advance Western Blot stripping kit (GM Biosciences, GM6031). Densitometry was performed using Multi Guage V3.0 software.

Chromatin Immunoprecipitation. ChIP assays were performed as described elsewhere (45). hCSCs were treated with either DMSO or PGE_2 (100 nM) for 24 h followed by fixing with formaldehyde. Immunoprecipitations were performed with either IgG or Acetylated Histone H3 antibodies (Millipore, 06–599). We used 5′GGTAGGCTACCAGCGGCTCT3′ and 5′-GTTCCCATCTCG-TAATCAGTGG-3′ oligonucleotides for amplification of region of interest in the 15-PGDH promoter (46).

siRNA-Mediated Knockdown. hCSCs were maintained in serum-free Opti MEM (11058-021, Life Technologies) overnight and transfected with 30 nM of either control negative siRNA (4390846, Ambion), HDAC2 siRNA (4390824, Ambion), HDAC4 siRNA (sc-35540, Santa Cruz Biotechnologies and 4392420, Ambion), or HDAC5 siRNA (4390824, Ambion) using Lipofectamine RNAimax Transfection reagent (13778-075) according to the supplier's protocol. Transfection medium was replaced with fresh DMEM with 10% FBS and incubated further for 24 h followed by a change to serum-free DMEM for 24 h. For quantifying basal levels of 15-PGDH, cells were further incubated for 12 h before processing for qRT-PCR. For different pharmacological treatments, cells were treated with either DMSO, PGE_2, or LMK-235 alone or PGE_2 + LMK-235 for 24 h in serum-free media.

Adenovirus-Mediated Overexpression. hCSCs grown in six-well dishes were infected with 5 μL (1×10^6 pfu/mL) of either β-galactosidase expressing control adenovirus (000197A, Applied Biological Materials Inc.) or HDAC4 expressing adenovirus (000426A, Applied Biological Materials Inc.) for 36 h in complete growth medium with 10% FBS followed by incubation in serum-free growth medium for 24 h before processing for qRT-PCR (no reverse transcriptase controls were included to confirm that RNA preparations were free from HDAC4 DNA from residual adenovirus in RNA preparations) and immunoblotting.

Immunocytochemistry. hCSCs were grown on tissue culture eight-chambered glass slides (4808, Lab-Tek) and treated with either DMSO or PGE_2 (100 nM) for 24 h. ICC was performed as described previously (47) with few modifications. Posttreatment cells were fixed with freshly prepared 4% formaldehyde for 15 min at room temperature. Cells were then rinsed with PBS three times (5 min each) to remove formaldehyde. Cells were then blocked using 10% normal goat serum (50062Z, ThermoFisher Scientific) in PBS with 0.3% Triton X-100 for 1 h at room temperature. After blocking, cells were incubated in anti-HDAC4 antibody (sc-11418, Santa Cruz Biotechnologies) diluted in PBS with 0.3% Triton X-100 overnight (dilution- 1:500) at 4 °C. After washing three times with fresh PBS for 5 min each, cells were then incubated with Alexa Fluor 488 goat anti-rabbit secondary antibody (A11008, Molecular Probes by Invitrogen) diluted in PBS with 0.3% Triton X-100 (1:500) for 1 h at room temperature in the dark. Cells were then washed three times with PBS (5 min each) and mounted with DAPI (P36395, Molecular Probes by Invitrogen), coverslipped, and imaged using a Leica TCS SP5 confocal microscope. Treatments were performed on the same slide, and images were captured with identical settings. Negative controls consisted of cells undergoing identical procedures with nonspecific IgG substituted for the primary antibody. Fluorescence was absent in these negative controls.

Immunohistochemistry. Formalin-fixed, paraffin-embedded tissues were sectioned at 5 μm and mounted on slides. Tissue sections from positive and negative sections were mounted on the same slide (48). Sections were immunostained with antibodies against HDAC4 (1:150, sc-11418, Santa Cruz Biotechnologies) in EDTA buffer using heated steam as the antigen retrieval method. Immunostaining was negative in controls in which tissues underwent all treatments except without primary antibody.

Animals and Treatments. To precisely determine the duration of gestation, C57BL/6 mice (with a gestation duration of 19 d) were time mated for 4 h (9:00 AM to 1:00 PM), after which females were separated from the males (day 0) and randomly divided into four treatment groups: (*i*) vehicle [88.33% D5W (5% Dextrose in water), 6.66% Ethyl alcohol, 3.33% Kolliphor EL (#C5135, Sigma), 1.66% DMSO], (*ii*) PGE_2 (1.68 mg/kg), (*iii*) SW033291 (2.5 mg/kg), and (*iv*) PGE_2 + SW033291. Reagents were freshly prepared each time just before treatment, and 300 μL was injected i.p. using a 28G needle, every 12 h (9:30 AM and 9:30 PM) starting on day 15 and observed for time of delivery using camera surveillance. Treatment was terminated on appearance of first pup, and the time of delivery was recorded for each treated animal. Final concentrations of vehicle components were similar in all treatment groups. Separate treatment groups were used for histology and biomechanics. Cervices were collected from different treatment groups on d 16 36 h posttreatment.

Histology. Tissues were harvested from three animals per treatment group on gestation d 16. The female reproductive tract containing the vagina, cervix, bifurcation of the uterus, and two lower pups were fixed in neutral=buffered formalin for 24 h. Thereafter, the buffer was changed to 50% ethanol and embedded in paraffin. Transverse serial sections from the external cervical os were obtained every 500 μm, and Masson's trichrome staining was performed.

Biomechanical Testing. Each cervix was suspended between two stainless steel wire mounts inserted through the cervical os and attached to a steel rod apparatus with a calibrated mechanical drive and to a force transducer (49–51). Tissues were maintained in a physiologic salt solution in water baths at 37 °C with 95% O_2 and 5% CO_2. After acclimation for 15 min, each ring was equilibrated to slack length (ring diameter at resting tone) as measured by the calibrated mechanical drive. Rings were distended in 1-mm increments with 2-min intervals between each increment to allow stabilization of forces before subsequent distention. This process was continued until failure (breakage) or until plateau of force generation. Force in Newtons was plotted against deformation, producing a sigmoid-shaped curve. Distensibility was considered the inverse of tissue stiffness, which was calculated from the slope of the linear portion of the curve.

Statistical Analysis. RNA-seq data were analyzed as described above. Otherwise, for multiple groups, ANOVA followed by Dunnett's post hoc testing (vehicle as control) was used except for gestational timing, in which an ANOVA was used followed by Tukey's post hoc testing. Student's *t* test was used to compare two independent groups.

Study Approval. Cervical tissues were obtained from women undergoing hysterectomy for benign gynecological conditions unrelated to cervical disease under a protocol approved by the Institutional Review Board at the University of Texas Southwestern Medical Center, with informed consent from all patients. Experimental protocols on animals were approved by the Institutional Animal Care and Use Committee of Texas Southwestern Medical Center.

ACKNOWLEDGMENTS. We acknowledge the helpful assistance of Parkland Hospital for tissue acquisition. C.X. was funded by NIH Grant UL1TR001105. S.W. was funded by the Council Advance Scholar Innovator Award from the Harrington Discovery Institute. This work was funded by NIH Grants HD080776 and HD082502 and March of Dimes Foundation Grant 21-FY-138 (to R.A.W.). Human cervical tissues were obtained from the Human Reproductive Tissue Core Laboratory funded by NIH Grant P01HD087150 (to R.A.W.).

1. Kelly AJ, Kavanagh J, Thomas J (2003) Vaginal prostaglandin (PGE2 and PGF2a) for induction of labour at term. *Cochrane Database Syst Rev* (4):CD003101.
2. Melamed N, Ben-Haroush A, Kremer S, Hod M, Yogev Y (2010) Failure of cervical ripening with prostaglandin-E2 can it be predicted? *J Matern Fetal Neonatal Med* 23: 536–540.
3. Anonymous (2008) *NICE Clinical Guidelines, No. 70. National Collaborating Centre for Women's and Children's Health (UK)* (RCOG Press, London, UK), Vol 8.
4. Challis JR, Patel FA, Pomini F (1999) Prostaglandin dehydrogenase and the initiation of labor. *J Perinat Med* 27:26–34.
5. Kishore AH, Owens D, Word RA (2014) Prostaglandin E2 regulates its own inactivating enzyme, 15-PGDH, by EP2 receptor-mediated cervical cell-specific mechanisms. *J Clin Endocrinol Metab* 99:1006–1018.
6. Törnblom SA, et al. (2004) 15-hydroxyprostaglandin dehydrogenase and cyclooxygenase 2 messenger ribonucleic acid expression and immunohistochemical

localization in human cervical tissue during term and preterm labor. *J Clin Endocrinol Metab* 89:2909–2915.
7. Havelock JC, et al. (2005) Human myometrial gene expression before and during parturition. *Biol Reprod* 72:707–719.
8. Loudon JA, Groom KM, Bennett PR (2003) Prostaglandin inhibitors in preterm labour. *Best Pract Res Clin Obstet Gynaecol* 17:731–744.
9. Olson DM, Ammann C (2007) Role of the prostaglandins in labour and prostaglandin receptor inhibitors in the prevention of preterm labour. *Front Biosci* 12:1329–1343.
10. Zuo J, Lei ZM, Rao CV, Pietrantoni M, Cook VD (1994) Differential cyclooxygenase-1 and -2 gene expression in human myometria from preterm and term deliveries. *J Clin Endocrinol Metab* 79:894–899.
11. Gross G, et al. (2000) Inhibition of cyclooxygenase-2 prevents inflammation-mediated preterm labor in the mouse. *Am J Physiol Regul Integr Comp Physiol* 278: R1415–R1423.
12. Rac VE, et al. (2007) Dose-dependent effects of meloxicam administration on cyclooxygenase-1 and cyclooxygenase-2 protein expression in intrauterine tissues and fetal tissues of a sheep model of preterm labor. *Reprod Sci* 14:750–764.
13. Fogg PC, et al. (2014) Class IIa histone deacetylases are conserved regulators of circadian function. *J Biol Chem* 289:34341–34348.
14. Backlund MG, et al. (2008) Repression of 15-hydroxyprostaglandin dehydrogenase involves histone deacetylase 2 and snail in colorectal cancer. *Cancer Res* 68: 9331–9337.
15. Tong M, Ding Y, Tai HH (2006) Histone deacetylase inhibitors and transforming growth factor-beta induce 15-hydroxyprostaglandin dehydrogenase expression in human lung adenocarcinoma cells. *Biochem Pharmacol* 72:701–709.
16. Wang X, et al. (2013) Combined histone deacetylase and cyclooxygenase inhibition achieves enhanced antiangiogenic effects in lung cancer cells. *Mol Carcinog* 52: 218–228.
17. Reader J, Holt D, Fulton A (2011) Prostaglandin E2 EP receptors as therapeutic targets in breast cancer. *Cancer Metastasis Rev* 30:449–463.
18. Axelsson H, Lönnroth C, Wang W, Svanberg E, Lundholm K (2005) Cyclooxygenase inhibition in early onset of tumor growth and related angiogenesis evaluated in EP1 and EP3 knockout tumor-bearing mice. *Angiogenesis* 8:339–348.
19. Backs J, Song K, Bezprozvannaya S, Chang S, Olson EN (2006) CaM kinase II selectively signals to histone deacetylase 4 during cardiomyocyte hypertrophy. *J Clin Invest* 116: 1853–1864.
20. Zhang X, et al. (2005) Histone deacetylase 3 (HDAC3) activity is regulated by interaction with protein serine/threonine phosphatase 4. *Genes Dev* 19:827–839.
21. Grozinger CM, Schreiber SL (2000) Regulation of histone deacetylase 4 and 5 and transcriptional activity by 14-3-3-dependent cellular localization. *Proc Natl Acad Sci USA* 97:7835–7840.
22. Paroni G, et al. (2008) PP2A regulates HDAC4 nuclear import. *Mol Biol Cell* 19: 655–667.
23. Little GH, Bai Y, Williams T, Poizat C (2007) Nuclear calcium/calmodulin-dependent protein kinase IIdelta preferentially transmits signals to histone deacetylase 4 in cardiac cells. *J Biol Chem* 282:7219–7231.
24. Dobrowsky RT, Kamibayashi C, Mumby MC, Hannun YA (1993) Ceramide activates heterotrimeric protein phosphatase 2A. *J Biol Chem* 268:15523–15530.
25. Zhang Y, et al. (2015) TISSUE REGENERATION. Inhibition of the prostaglandin-degrading enzyme 15-PGDH potentiates tissue regeneration. *Science* 348:aaa2340.
26. Sadowsky DW, Haluska GJ, Gravett MG, Witkin SS, Novy MJ (2000) Indomethacin blocks interleukin 1beta-induced myometrial contractions in pregnant rhesus monkeys. *Am J Obstet Gynecol* 183:173–180.
27. Giannoulias D, et al. (2005) Localization of prostaglandin H synthase, prostaglandin dehydrogenase, corticotropin releasing hormone and glucocorticoid receptor in rhesus monkey fetal membranes with labor and in the presence of infection. *Placenta* 26:289–297.
28. Gravett MG, et al. (2007) Immunomodulators plus antibiotics delay preterm delivery after experimental intraamniotic infection in a nonhuman primate model. *Am J Obstet Gynecol* 197:518.e1–518.e8.
29. Yokoyama U, et al. (2014) Prostaglandin E2 inhibits elastogenesis in the ductus arteriosus via EP4 signaling. *Circulation* 129:487–496.
30. Yokoyama U, et al. (2006) Chronic activation of the prostaglandin receptor EP4 promotes hyaluronan-mediated neointimal formation in the ductus arteriosus. *J Clin Invest* 116:3026–3034.
31. Fang D, et al. (2015) Direct electrical stimulation softens the cervix in pregnant and nonpregnant rats. *Am J Obstet Gynecol* 212:786.e1–786.e9.
32. Roizen JD, Asada M, Tong M, Tai HH, Muglia LJ (2008) Preterm birth without progesterone withdrawal in 15-hydroxyprostaglandin dehydrogenase hypomorphic mice. *Mol Endocrinol* 22:105–112.
33. Condon JC, Jeyasuria P, Faust JM, Wilson JW, Mendelson CR (2003) A decline in the levels of progesterone receptor coactivators in the pregnant uterus at term may antagonize progesterone receptor function and contribute to the initiation of parturition. *Proc Natl Acad Sci USA* 100:9518–9523.
34. Ganesh T, Jiang J, Dingledine R (2014) Development of second generation EP2 antagonists with high selectivity. *Eur J Med Chem* 82:521–535.
35. Wingerup L, Andersson KE, Ulmsten U (1978) Ripening of the uterine cervix and induction of labour at term with prostaglandin E2 in viscous gel. *Acta Obstet Gynecol Scand* 57:403–406.
36. Andersson S, Minjarez D, Yost NP, Word RA (2008) Estrogen and progesterone metabolism in the cervix during pregnancy and parturition. *J Clin Endocrinol Metab* 93: 2366–2374.
37. Wang L, et al. (2011) A low-cost library construction protocol and data analysis pipeline for Illumina-based strand-specific multiplex RNA-seq. *PLoS One* 6:e26426.
38. Trapnell C, et al. (2012) Differential gene and transcript expression analysis of RNA-seq experiments with TopHat and Cufflinks. *Nat Protoc* 7:562–578.
39. Liao Y, et al. (2014) FeatureCounts: An efficient general purpose program for assigning sequence reads to genomic features. *Bioinformatics* 30(7):923–930.
40. McCarthy DJ, et al. (2012) Differential expression analysis of multifactor RNA-Seq experiments with respect to biological variation. *Nucleic Acids Res* 40(10):4288–4297.
41. Huang da W, et al. (2009) Systematic and integrative analysis of large gene lists using DAVID bioinformatics resources. *Nat Protoc* 4(1):44–57.
42. Huang da W, et al. (2009) Bioinformatics enrichment tools: paths toward the comprehensive functional analysis of large gene lists. *Nucleic Acids Res* 37(1):1–13.
43. Chirgwin JM, Przybyla AE, MacDonald RJ, Rutter WJ (1979) Isolation of biologically active ribonucleic acid from sources enriched in ribonuclease. *Biochemistry* 18: 5294–5299.
44. Hari Kishore A, Li XH, Word RA (2012) Hypoxia and PGE(2) regulate MiTF-CX during cervical ripening. *Mol Endocrinol* 26:2031–2045.
45. Li XH, et al. (2010) A novel isoform of microphthalmia-associated transcription factor inhibits IL-8 gene expression in human cervical stromal cells. *Mol Endocrinol* 24: 1512–1528.
46. Wolf I, et al. (2006) 15-hydroxyprostaglandin dehydrogenase is a tumor suppressor of human breast cancer. *Cancer Res* 66:7818–7823.
47. Mogami H, et al. (2013) Fetal fibronectin signaling induces matrix metalloproteases and cyclooxygenase-2 (COX-2) in amnion cells and preterm birth in mice. *J Biol Chem* 288:1953–1966.
48. Miller RT, Groothuis CL (1991) Multitumor "sausage" blocks in immunohistochemistry. Simplified method of preparation, practical uses, and roles in quality assurance. *Am J Clin Pathol* 96:228–232.
49. Mahendroo MS, Porter A, Russell DW, Word RA (1999) The parturition defect in steroid 5alpha-reductase type 1 knockout mice is due to impaired cervical ripening. *Mol Endocrinol* 13:981–992.
50. Read CP, Word RA, Ruscheinsky MA, Timmons BC, Mahendroo MS (2007) Cervical remodeling during pregnancy and parturition: Molecular characterization of the softening phase in mice. *Reproduction* 134:327–340.
51. Word RA, Landrum CP, Timmons BC, Young SG, Mahendroo MS (2005) Transgene insertion on mouse chromosome 6 impairs function of the uterine cervix and causes failure of parturition. *Biol Reprod* 73:1046–1056.